Shock-Induced Transformation of Liquid Deuterium into a Metallic Fluid

P. M. Celliers, G. W. Collins, L. B. Da Silva, D. M. Gold, R. Cauble, R. J. Wallace, M. E. Foord, and B. A. Hammel
Lawrence Livermore National Laboratory, P.O. Box 808, Livermore, California 94551
(Received 9 November 1999)

Simultaneous measurements of shock velocity and optical reflectance at 1064, 808, and 404 nm of a high pressure shock front propagating through liquid deuterium show a continuous increase in reflectance from below 10% and saturating at $\sim(40-60)\%$ in the range of shock velocities from 12 to 20 μm/ns (pressure range 17–50 GPa). The high optical reflectance is evidence that the shocked deuterium reaches a conducting state characteristic of a metallic fluid. Above 20 μm/ns shock velocity (50 GPa pressure) reflectance is constant indicating that the transformation is substantially complete.

PACS numbers: 71.30.+h, 62.50.+p, 64.30.+t

Hydrogen at high pressures and modest temperatures is of great current scientific interest. Monte Carlo simulations have recently predicted that dense fluid hydrogen undergoes a first-order transition to conducting states with critical point at $\sim$50 GPa and $\sim$10 000 K [1]. The first observation of a metallic phase of hydrogen at high pressure was recently reported at 140 GPa and $\sim$3000 K by Weir *et al.* [2,3]. Recent experiments using an intense laser to compress deuterium up to 300 GPa have reported sixfold compression on the principal Hugoniot above 25 GPa [4,5]. This unexpectedly large compression was attributed to continuous dissociation of the molecular fluid into a monatomic metallic fluid. The properties of hydrogen at these conditions are necessary constituents of models of planetary interiors [6–8] and have important practical applications for inertial confinement fusion [9,10]. In order to determine where shock-compressed fluid hydrogen becomes conducting we have measured the optical reflectance of the shock front over a range of pressures from 20–500 GPa.

The experimental arrangement for measuring laser-driven shock waves in liquid deuterium is similar to that described previously [4,5]. Using the Nova laser [11] we generated a high pressure shock wave in a pusher material (either Al or Be) using either direct laser irradiation of the pusher with one beam of Nova, or by soft x-ray irradiation using a hohlraum radiation cavity [9] heated by five beams. Behind the pusher was a volume filled with the liquid deuterium sample at density 0.17 g cm^{-3} and temperature 20 K. The shock wave transmitted through the pusher released into the liquid and generated a shock in the deuterium. Additional Nova beam(s) generated an x-ray source that allowed us to radiograph the positions of the shock front and the pusher-deuterium interface as a function of time (see Fig. 3 in Ref. [4]). From this information we determined the pressure and density in the shock-compressed fluid using the Rankine-Hugoniot relations [12].

To investigate the metallic transition in shocked deuterium we probed the reflectance of the shock front at normal incidence using a 15-ns-duration laser pulse from an injection-seeded Q-switched laser as a probe. We obtained simultaneous shock velocity and reflectance data with two lasers: a Nd:YAG operating at 1064 nm and a Ti:sapphire operating at 808 nm and at its second harmonic, 404 nm. A 150-mm focal length $f/3$ objective imaged the reflected light into a velocity interferometer [13] and the image was further relayed onto the slit of a streak camera. The streak camera captured a time- and space-resolved recording of the light reflected from the sample. Details of this experimental arrangement are presented elsewhere [14].

Figure 1 shows two example data records. The fringe pattern is produced by the velocity interferometer. Frequency shifts in the light passing through the interferometer cause proportional fringe shifts. Before the shock emerges from the pusher into the sample ($t < 0$) the reflection originates at the stationary pusher-sample interface, and the fringe phase is constant. When the shock emerges from the pusher into the sample ($t = 0$) the reflected intensity drops simultaneously with a fringe shift—owing to the Doppler shift from the moving reflector (the shock front). We determine the shock velocity ($t > 0$) by measuring the fringe phase. We have verified that for $t > 0$ the reflection originates from the shock front: Integration of the velocity inferred from the fringe phase reproduced the shock trajectory (position as a function of time) observed simultaneously using the x-ray radiographic measurement [14]. We determine the shock reflectance relative to that of the pusher from the intensities reflected from the pusher ($t < 0$) and the shock ($t > 0$). In a separate calibration we measured the absolute reflectances of several representative pusher samples and found them to be in good agreement with handbook values [15,16]: $(90 \pm 10)\%$, $(80 \pm 10)\%$, and $(70 \pm 10)\%$ for the Al pushers at 1064, 808, and 404 nm, respectively (diamond turned substrates); and $(33 \pm 5)\%$ for Be pushers at 1064 nm (machined substrates).

The experiment in Fig. 1(a) produced a steady shock: At $t = 0$ there is a 40% drop in intensity accompanied by a fringe shift. The points in Fig. 2 are from a series of such measurements for several drive conditions and pusher types producing shock speeds from 17 to 62 μm/ns, corresponding to pressures from 40 to 500 GPa. In a different kind of experiment we irradiated the pusher with a short

 0031-9007/00/84(24)/5564(4)$15.00

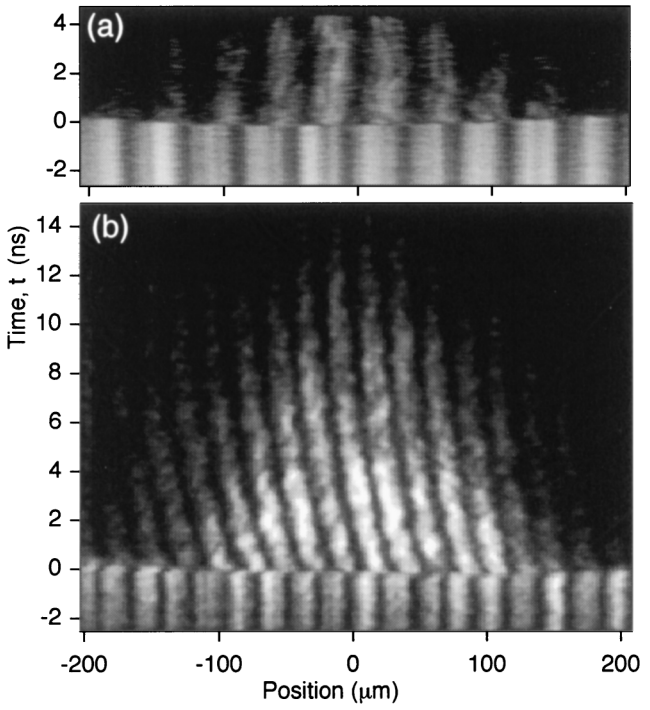

FIG. 1. Light at 1064-nm wavelength reflected from a shock front in deuterium observed through the velocity interferometer (a) for a steady shock and (b) for an attenuating shock. At $t = 0$ the shock was transmitted from the pusher into the liquid sample. The phase of the fringe pattern is proportional to the shock velocity. In (a) the reflected signal decreased to 61% of its initial value at $t = 0$ (reflectance ~55%) and the shock speed was 23 μm/ns (the phase shifted 1.2 fringes to the right). In (b) the initial shock speed was 20 μm/ns (initial phase shift 3.3 fringes); the fringes shifted continuously to the left (deceleration) as the shock decayed; reflectance decreases simultaneously. The images do not show reflectance directly: in (b) the illumination pulse reached its peak at $t \sim 5$ ns and remained above 30% of its peak power for $5 < t < 15$ ns.

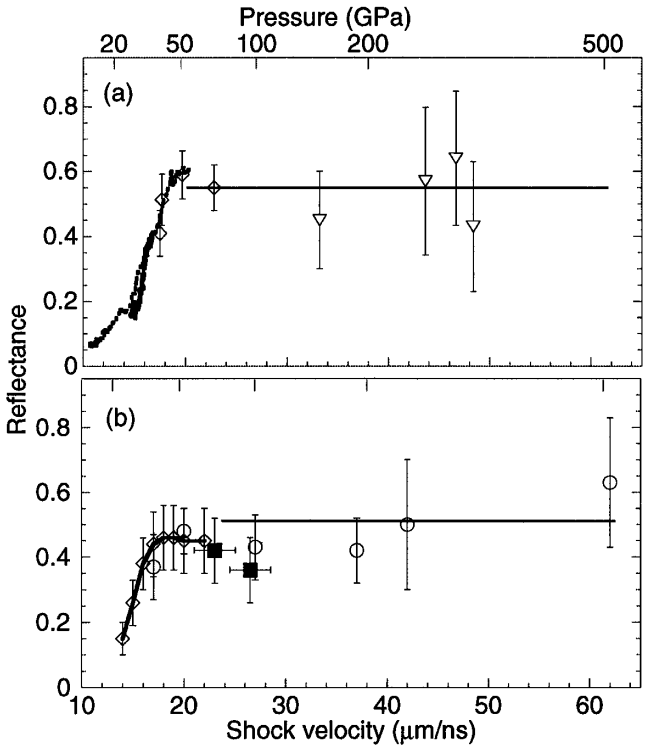

FIG. 2. Shock front reflectance as a function of shock velocity. The indicated pressures were determined from Hugoniot data. Velocity uncertainty where no errors are indicated is better than ± 1 μm/ns. (a) Measurements at 1064 nm: open symbols show single-point measurements at shock breakout from Al pushers (diamonds) and Be pushers (triangles). The Be pusher surfaces were rougher than the Al surfaces producing more scatter and larger uncertainty. The dotted curve was extracted from the record shown in Fig. 1(b), and the solid curve from a similar experiment. The horizontal line is placed at $R = 55\%$ (our Drude estimate). (b) Reflectance at 808 nm for steady shocks (open circles) and an attenuating shock (open diamonds on curve) and at 404 nm (solid squares) for a similar range of shock velocities as in (a). The horizontal line is placed at $R = 51\%$.

(1 ns) high pressure pulse, which produced an attenuating shock in the sample [see Fig. 1(b)]. Clearly observable is a continuous fringe shift accompanied by a decrease in reflected intensity as the shock attenuated. This experiment yielded a continuous record of reflectance versus shock velocity through a velocity range from 12 to 20 μm/ns. The data from attenuating shocks are shown as curves in Fig. 2.

The lowest observed shock speeds at 1064 nm, 11 μm/ns yielded ~6% reflectance; at 808 nm we observed ~15% reflectance at 14 μm/ns. From 12–20 μm/ns (17–50 GPa pressure [4,5,17]) the data show a continuously increasing reflectance, above which it saturates at a constant level (observed up to 500 GPa). Saturation levels are ~55% at 1064 nm, ~45% at 808 nm, and ~40% at 404 nm (two data points around 24 μm/ns).

The width of a strong shock in dense fluids is of the order of 1–2 nm (a few dozen atomic spacings) [18]. Optical measurements of strongly shocked dielectrics show that the shock front is a specular reflector, and its reflectivity is amenable to Fresnel analysis [19]. The Fresnel formula for the reflectivity of the shock front is $R = |(\hat{n}_s - n_0)/(\hat{n}_s + n_0)|^2$, where $\hat{n}_s$ is the (complex) refractive index behind the shock front and $n_0 = 1.13$ is the refractive index in the undisturbed liquid. At low pressures the refractive index of cryogenic liquid deuterium follows an empirical Gladstone-Dale form, $n - 1 \propto \rho$, where ρ is the density [20]. This scaling has also been found to describe the density dependence of the refractive index for many dielectric liquids under shock compression [19,21]. Assuming the Gladstone-Dale scaling and that the fluid remains mostly in its molecular form under shock compression, the refractive index at sixfold compression would be $\hat{n}_s \sim 1.8$, and the reflectivity ~5%. The much higher reflectances we observe suggest that the fluid becomes conducting: The transformation to the conducting state is continuous beginning around 20 GPa and reaches completion around 50 GPa. At extreme shock pressures (exceeding 200 GPa) the observation of metallic conduction in the shocked fluid is expected. All theoretical equation-of-state

models of hydrogen incorporate some description of the transformation from the insulating molecular fluid to a conducting phase. However, there is great variance in the theoretical predictions of the shock compression curve and in the nature of the transformation to the conducting phase [5]. The greatest theoretical variations exist in the 20–200 GPa pressure range.

Using an optical pyrometer we have measured temperature of shocked deuterium [22]; at 50 GPa the temperature is ~8000 K. If we assume the conducting state is a monatomic metallic fluid, then the Fermi energy varies from 12 to 16 eV over the densities produced in the experiment; at this temperature the fluid is partially degenerate, similar to a liquid metal. Drude-type models are often applied to parametrize the optical properties of liquid metals [23]. The fact that we observe similar reflectances at wavelengths spanning the visible spectrum (from 400 to 1064 nm) is consistent with a Drude-type optical response. Within the Drude description the complex index of refraction is given by $\hat{n}_s^2 = 1 - (\omega_p^2/\omega^2)(1 + i/\omega\tau_e)^{-1}$, where ω is the optical frequency, ω_p is the plasma frequency, and τ_e is the electron relaxation time. The two latter parameters characterize the metallic state. The plasma frequency is related to the density of conducting states near the Fermi surface and can be expressed as $\omega_p^2(n_e) = 4\pi n_e e^2/m_e$, where n_e is an effective carrier density, and e and m_e are the electronic charge and effective electron mass, respectively. Using the observed reflectances as a guide we can estimate the values of both parameters.

The most prominent feature of the Drude model is the absorption edge where the optical frequency matches the plasma frequency. This condition implicitly defines the critical density n_c: $\omega_p^2(n_c) = \omega^2$. For the optical wavelengths of 1064, 808, and 404 nm, $n_c = 10^{21}$, 1.7×10^{21}, and 6.8×10^{21} cm^{-3}, respectively. High reflectances cannot be produced at carrier densities $n_e < n_c$, independent of τ_e. We will justify below that the data suggest strong electron scattering such that $\omega\tau_e \sim 0.1$ for visible and infrared wavelengths (metals usually exhibit $\omega\tau_e \geq 1$ at these wavelengths). For $\omega\tau_e \ll 1$ an examination of Fresnel reflectivity with the Drude model shows that significant reflectivities are produced only when $n_e/n_c \geq 2/\omega\tau_e$ or larger, i.e., that $n_e \sim 10^{22}$–10^{23} cm^{-3} is required to account for the observations. Based on electrical conductivity measurements of deuterium shocked to 20 GPa (near our lowest pressures), Nellis *et al.* [24] estimated a carrier concentration of 10^{15} cm^{-3} (0.0001% ionization) in fluid that is still mostly molecular. This carrier density would produce little observable reflectivity; at similar conditions we observed reflectance <8%. Therefore, the reflectances we observe at higher pressures must come about through a large increase in the carrier concentration: some 7 to 8 orders of magnitude in the 20–50 GPa pressure range on the Hugoniot.

Electron relaxation times in fluid systems undergoing metal-insulator transitions often take on values near the Ioffe-Regel limit [25]. In this limit one can characterize the relaxation time through the expression $\tau_e = R_0/\nu_f$, where ν_f is the electron Fermi speed, and R_0 is the interparticle spacing [26]. This limit applies to strongly scattering disordered systems and leads to the minimum conductivity of a metal. The dc conductivity of hydrogen measured by Weir *et al.* at higher density and lower temperature than our measurements is also consistent with the Ioffe-Regel limit [3]. Therefore we will assume that in the shocked fluid with temperatures around 0.5–1 eV, the Ioffe-Regel limit provides a reasonable estimate of τ_e. Between 60 and 200 GPa shock densities are approximately constant, varying between 0.9 and 1.0 g cm^{-3} (shock velocity ranges between 20 and 40 μm/ns). At a density of 1 g cm^{-3}, monatomic metallic deuterium will produce a carrier density of 3×10^{23} cm^{-3}, and the Ioffe-Regel condition predicts $\tau_e = 4.9 \times 10^{-17}$ s. This yields $\omega\tau_e \sim 0.09$ and $R = 55\%$ at 1064 nm, $\omega\tau_e \sim 0.11$ and $R = 51\%$ at 808 nm, and $\omega\tau_e = 0.23$ and $R = 40\%$ at 404 nm. These estimated reflectivities are consistent with our observations. Theoretical calculations of the electrical conductivity of dense hydrogen plasmas [27] give $\sigma_0 \sim 10^5$ $(\Omega\,\text{cm})^{-1}$ corresponding to $\omega\tau_e \sim 2$ at 1064 nm, similar to alkali metal conductivities. With the Drude model this conductivity would produce >95% reflectivity, more than twice the level we observe.

Figure 3 shows estimates of the Drude reflectivity of fluid metallic deuterium as a function of n_e with the relaxation time set at the Ioffe-Regel limit, i.e., with $\tau_e = R_0/\nu_f(n_e)$. We set $R_0 = 0.12$ nm corresponding to a density of 1 g cm^{-3}. The predicted reflectivity is nearly independent of wavelength and the value at $n_e \sim 3 \times 10^{23}$ cm^{-3} (full ionization) saturates at (40–55)%, consistent with observation. At $n_e = 10^{23}$ cm^{-3} the Fermi

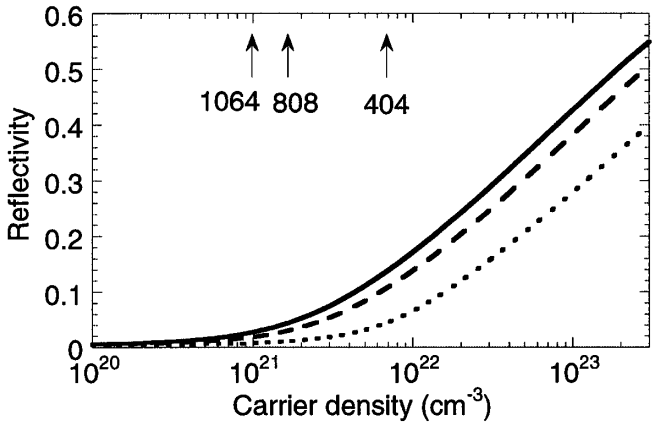

FIG. 3. Drude reflectivity at the Ioffe-Regel limit [$\tau_e = R_0/\nu_f(n_e)$] with $R_0 = 0.12$ nm plotted as a function of carrier density: at 1064 nm (solid line), 808 nm (dashed line), and 404 nm (dotted line). Critical densities are indicated for each wavelength by the arrows.

energy is 8 eV, more than 10 kT at 60 GPa on the Hugoniot and therefore still consistent with our assumption of degenerate conditions. Towards the strong shock extreme of our observations, the data suggest that the reflectance begins to increase (shock velocity >60 μm/ns, $P > 500$ GPa); at these conditions shock temperatures exceed 10 eV, comparable to the Fermi temperature, thus lifting the degeneracy and approaching a dense plasma state.

The transformation to conducting states we observe occurs at significantly lower pressures and densities than the metallized state produced in the experiments of Weir *et al.*, although our temperatures are much higher. One might consider whether thermal excitations are sufficient to account for the observed reflectances within the context of the findings of Weir *et al.* From dc electrical conductivity measurements of hydrogen and deuterium compressed by single shocks (to 20 GPa) [24] and multiple-reverberating shocks (to 140 GPa) [2] Nellis *et al.* inferred the density dependent mobility gap energy (E_g) of the semiconducting *molecular* fluid [3]. According to their findings metallization takes place when the $E_g \sim$ kT; the gap closes at ~ 1.2 g cm^{-3} (for deuterium). The rising reflectance we observe takes place at densities much *less* than this. At 30 GPa shock pressure the density is ~ 0.7 g cm^{-3} (reflectance $\sim 25\%$ at 1064 and 808 nm) and $E_g \sim 9$ eV $\sim$ 13 kT. Since $E_g \gg$ kT and $E_g \gg \hbar\omega$ electronic excitations in the semiconducting phase cannot account for metallic reflectances. However, in our density range the estimated energy for molecular dissociation (E_{dis}) into the monatomic phase [3,28] is much lower than E_g: $E_{\mathrm{dis}} \sim$ 3 eV $\sim$ 4 kT. The higher temperatures in our experiments drive dissociation and each monomer contributes a delocalized electron, leading to metallic carrier densities around 10^{23} cm^{-3}.

The high compressibility previously observed on the principal Hugoniot [4,5] was interpreted as a result of the dissociation of the molecular fluid into the monatomic metallic fluid phase. Two phenomenological models by Ross [28] and by Saumon, Chabrier, and Van Horn [29] predict similar shock compressibilities (through dissociation) and predict carrier densities $\sim 10^{23}$ cm^{-3} in the fluid metallic phase. We find no evidence of discontinuous behavior in the reflectance as a function of shock velocity, such as might be expected if the metallization occurred through a first-order phase transition.

We thank J. R. Asay, N. W. Ashcroft, N. C. Holmes, W. J. Nellis, A. Ng, M. Ross, and T. Tajima for useful discussions and B. T. Goodwin, J. K. Kilkenny, and L. T. Wiley for support of this work. This work was performed under the auspices of the U.S. D.O.E. by LLNL under Contract No. W-7405-ENG-48.

[1] W. R. Magro, D. M. Ceperley, C. Pierleoni, and B. Bernu, Phys. Rev. Lett. **76**, 1240–1243 (1996).
[2] S. T. Weir, A. C. Mitchell, and W. J. Nellis, Phys. Rev. Lett. **76**, 1860–1863 (1996).
[3] W. J. Nellis, S. T. Weir, and A. C. Mitchell, Phys. Rev. B **59**, 3434–3449 (1999).
[4] L. B. Da Silva *et al.*, Phys. Rev. Lett. **78**, 483–486 (1997).
[5] G. W. Collins *et al.*, Science **281**, 1178–1181 (1998).
[6] W. B. Hubbard, Science **214**, 145–149 (1981).
[7] D. J. Stevenson, Rep. Prog. Phys. **46**, 555–620 (1983).
[8] T. Guillot, Science **286**, 72–77 (1999).
[9] J. Lindl, Phys. Plasmas **2**, 3933–4024 (1995).
[10] S. W. Haan *et al.*, Phys. Plasmas **2**, 2480–2487 (1995).
[11] E. M. Campbell, Laser Part. Beams **9**, 209–231 (1991).
[12] Y. B. Zel'dovich and Y. P. Raizer, *Physics of Shock Waves and High-Temperature Hydrodynamic Phenomena* (Academic Press, New York, 1966).
[13] L. M. Barker and R. E. Hollenbach, J. Appl. Phys. **43**, 4669–4675 (1972).
[14] P. M. Celliers *et al.*, Appl. Phys. Lett. **73**, 1320–1322 (1998).
[15] D. Y. Smith, E. Shiles, and M. Inokuti, in *Handbook of Optical Constants of Solids*, edited by E. D. Palik (Academic Press, Orlando, 1985), pp. 369–406.
[16] E. T. Arakawa, T. A. Callcott, and Y.-C. Chang, in *Handbook of Optical Constants of Solids*, edited by E. D. Palik (Academic Press, Boston, 1991), Vol. II, pp. 421–433.
[17] W. J. Nellis *et al.*, J. Chem. Phys. **79**, 1480–1486 (1983).
[18] W. G. Hoover, Phys. Rev. Lett. **42**, 1531–1534 (1979).
[19] S. B. Kormer, Sov. Phys. Usp. **11**, 229–254 (1968).
[20] P. C. Souers, *Hydrogen Properties for Fusion Energy* (University of California, Berkeley, 1986).
[21] D. R. Hardesty, J. Appl. Phys. **47**, 1994–1998 (1976).
[22] G. W. Collins *et al.* (to be published).
[23] J. N. Hodgson, in *Liquid Metals, Chemistry and Physics*, edited by S. Z. Beer (Marcel Dekker, New York, 1972).
[24] W. J. Nellis *et al.*, Phys. Rev. Lett. **68**, 2937–2940 (1992).
[25] F. Hensel and P. Edwards, Phys. World **9**, 43–46 (1996); F. Hensel and W. W. Warren, Jr., *Fluid Metals: The Liquid-Vapor Transition of Metals* (Princeton University Press, Princeton, 1999).
[26] A. F. Ioffe and A. R. Regel, Prog. Semicond. **4**, 237 (1960).
[27] W. B. Hubbard and M. Lampe, Astrophys. J. Suppl. **18**, 297–346 (1969).
[28] M. Ross, Phys. Rev. B **58**, 669–677 (1998).
[29] D. Saumon, G. Chabrier, and H. M. Van Horn, Astrophys. J. Suppl. **99**, 713–741 (1995).